NAL TR-1333T

ISSN 0389-4010
UDC 528. 27
528.024
629. 052

TECHNICAL REPORT OF NATIONAL AEROSPACE LABORATORY

TR-1333T

An Onboard Measurement System of Gravity Gradients Using Inertial Accelerometers

Hirokimi SHINGU

September 1997

NATIONAL AEROSPACE LABORATORY

CHŌFU, TOKYO, JAPAN

An Onboard Measurement System of Gravity Gradients Using Inertial Accelerometers*

Hirokimi SHINGU**

ABSTRACT

A method for onboard measurement of gravity gradients is proposed in this paper. First, the theory of a conservative field and its gradients is briefly reviewed, and analytical solutions of gravity gradients are derived as second-order spatial gradients of the gravitational potential in the conservative field, and the equation governing the relation among inertial and gravitational accelerations and size effect is derived. Next, it is shown that the gravity gradients can be obtained from the outputs of inertial accelerometers placed some distance away from each other, and the concept of the measurement system is clarified. It is then analytically shown that a gravity gradiometer system can be configured using twelve single-degree-of-freedom (SDF) accelerometers or six two-degree-of-freedom (TDF) accelerometers or four three-degree-of-freedom (THDF) accelerometers. The measurement accuracy related to the arrangement errors of each accelerometer is quantitatively evaluated. Then the applicability of the gravity gradiometer for a strapdown inertial navigation system is verified by simulation using the model of the moving vehicle. Finally, it is concluded that a new type of inertial navigation system using gravity gradiometers can be configured when it becomes possible to precisely measure gravity gradients.

Keywords: gravity potential, inertial sensor, accelerometer, inertial navigation

概　　要

本論文では，引力傾斜の機上計測を可能にする方法が提案されている。まず，保存力場とその傾斜に関する理論解析を通じて引力傾斜の解析解が引力ポテンシャルの２次の空間勾配として導出され，慣性加速度，引力加速度，サイズ効果の関係が明らかにされている。次に，ある間隔離して置かれた複数個の慣性加速度計の出力の差が引力傾斜になり得ることが解析的に示され，計測システムの構成概念が論じられてれている。12 個の１自由度加速度計または６個の２自由度加速度計または４個の３自由度加速度計を用いて，引力傾斜計のシステム構成が可能になることが明らかにされ，各構成において，加速度計の配置精度と引力傾斜の計測精度との関係が示されている。また，ストラップダウン慣性航法システムにおける引力変動の機上補正の有用性がシミュレーション結果に基いて評価されている。そして，この有用性評価をベースに，引力傾斜の計測精度の向上とともに，新しい型の慣性航法システムの構成が可能になると結論づけられている。

1. Introduction

An inertial navigation system utilizes the inertial properties of sensors mounted aboard the vehicle to execute the navigation function and is capable of continuous determinination of vehicle position and velocity without the use of external information. The sensors used in the conventional strapdown inertial navigation system are gyroscopes and accelerometers,which measure changes in the vehicle's heading and speed, respectively. These changes are caused by nongravitational forces. The gravitational field necessary for navigation computation is obtained by calcu-

＊　received 16 June 1997
＊＊　Control Systems Division

lations using the prescribed reference ellipsoid of the earth's geoid and the position vector of the vehicle. The reference ellipsoid gives a good representation of the overall shape of the geoid, but cannot account for local changes in gravity caused by geologic features and density variation within the earth's crust[1,2]. Thus there exist errors of gravity calculation based on the unpredictable behavior of the earth's gravity vector. In order to realize a more advanced inertial navigator, it is necessary to directly measure gravitational acceleration on a moving vehicle in real time. It is impossible to separate inertial and gravitational effects from the measured data of an acceleration at any one point in an inertial reference frame because the proof mass of an accelerometer reacts identically to inertial and gravitational accelerations. But a change in gravity can be obtained from the difference in gravitational acceleration between two points, because line inertial acceleration is the same throughout a vehicle but the gravitational acceleration is not. That is, the difference between two line inertial accelerations contained in the outputs of two accelerometers arrayed some distance away from each other is the gravity gradient corresponding to this distance. Line acceleration is defined as the quantity obtained by subtracting the size effect[3] from the accelerometer output in this paper. Size effect can be obtained from angular velocities and angular accelerations along three orthogonal directions. Accordingly, various types of gravity gradiometers can be realized using inertial accelerometers along with gyroscopes and angular accelerometers.

2. Definition of Gravity Gradient

The gravitational forces due to such bodies as the earth, the sun and the moon act on the vehicle in accordance with Newton's "Law of Universal Gravitation". The gravitational potential in the position of the vehicle is proportional to both the mass of each body and the inverse of the distance from each body. Here, the process of deriving the gravitational accelerations and gravity gradients from the gravitational potential is shown, briefly reviewing the theory of the conservative field, with definition of related coordinate systems. The position of the vehicle relative to other bodies including the earth is shown in Fig.1. O_e-XYZ is a reference coordinate system (= inertial frame in this study) and P_0-xyz is a body-fixed coordinate system. λ and η are the latitude and the longitude of the point P_0, respectively. Here, P_0 is the center of gravity of the vehicle. ω_e is earth's inertial angular velocity. M_e and M_b are the mass of the earth and the mass of the vehicle, respectively. $M_1, M_2, \cdots\cdots M_n$ are the masses of bodies excluding the earth, and $r_1, r_2, \cdots\cdots r_n$ are distances from the point P_0 to the points $O_1, O_2, \cdots\cdots O_n$ of bodies. These points are called

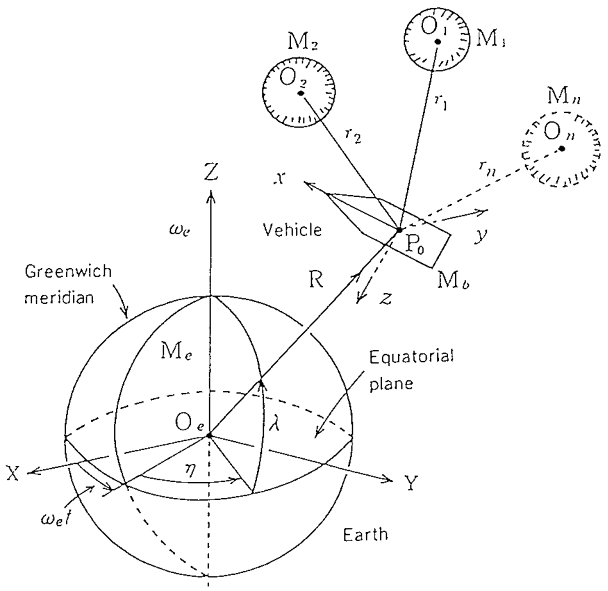

Fig. 1 Inertial Reference Coordinate (O_e-XYZ) and body-fixed coordinate (P_0-xyz)

"geometric center" here. The earth's center of mass is assumed to coincide with the geometric center and thus with the origin O_e of the inertial reference coordinate system. The components of the distance R from O_e to P_0 along O_eX, O_eY and O_eZ axes are expressed by R_X, R_Y and R_Z. The components of the distance R along P_{0x}, P_{0y} and P_{0z} axes are expressed by R_x, R_y and R_z. These R_x, R_y and R_z can be transformed to R_X, R_Y and R_Z using the direction cosine matrix $[C_{ij}]$.

$$[R_X\ R_Y\ R_Z]^T = [C_{ij}]\ [R_x\ R_y\ R_z]^T,\ i, j = 1, 2, 3 \tag{1}$$

The mass of the vehicle ($= M_b$) can be regarded as unit quantity for the purpose of discussing the gravitational field[4]. Total quantity of the gravitational potential at point P_0 of the vehicle is expressed as the scalar summation of the gravitational potentials due to all bodies including the earth with the masses of M_e, M_1, $M_2, \cdots\cdots M_n$, respectively. The gravitational potential is assumed to be evaluated at a point external to these bodies. If the geoids of all bodies are perfectly spherical and homogeneous and their mass centers coincide with the geometric centers $O_1, O_2, \cdots\cdots O_n$, the gravitational potential of the vehicle at point P_0 is defined as follows:

$$U = -\mu\frac{1}{R} - \mu_1\frac{1}{r_1} - \mu_2\frac{1}{r_2} - \mu_3\frac{1}{r_3} - \cdots \tag{2}$$

Here, μ is the product of the universal gravitational constant with the earth's mass M_e and $\mu_1, \mu_2, \mu_3, \cdots\cdots$ are the products of the universal gravitational constant with the masses $M_1, M_2, M_3, \cdots\cdots$ of other bodies. The gravitational field g is a vector field which is derived as the first partial derivative of the gravitational potential in each coordinate system. The components of g are g_X, g_Y, g_Z for the O_e-XYZ system and g_x, g_y, g_z for the P_0-xyz system. The gravity gradient with respect to the reference coordinate system is defined as follows:

$$[g_{ij}]=\left[\frac{\partial g_i}{\partial R_j}\right]=\left[\frac{\partial^2 U}{\partial R_i \partial R_j}\right],\quad i,j = X, Y, Z \qquad (3)$$

Here, $[g_{ij}]$ is the second order tensor of the potential U with respect to R_X, R_Y, R_Z. The data measured using the gravity gradiometer mounted in the vehicle are the components of the gravity gradient with respect to body-fixed coordinate system and is defined as follows:

$$[g_{nm}]=\left[\frac{\partial g_n}{\partial R_m}\right]=\left[\frac{\partial^2 U}{\partial R_n \partial R_m}\right],\quad n, m = x, y, z \qquad (4)$$

Here, $[g_{nm}]$ is the second order tensor of the potential U with respect to R_x, R_y, R_z. The gravity gradient tensors shown in Eqs. (3) and (4) are symmetric because the elements are the second order partial derivative of the gravity potential U. The following relations are easily obtained from Eqs. (3) and (4).

$$g_{ij} = g_{ji},\ g_{nm} = g_{mn},\ i, j = X, Y, Z,\quad n, m = x, y, z \qquad (5)$$

Applying Eqs. (1), (2) to Eqs. (3) and (4), the sum of the diagonal elements of each gradient tensor is as follows:

$$\Sigma g_{ii} = 0,\ \Sigma g_{nn} = 0,\ i = X, Y, Z,\ n = x, y, z \qquad (6)$$

Equations (5) and (6) show that it is necessary to determine five unknowns to describe the rate of change in gravity at a single point. That is, the total number of independent elements is reduced to five. Therefore, complete determination of the gravity gradient tensor at any point in space requires only five independent measurements.

3. Concept of Measurement System

It is shown here that the difference between gravitational accelerations at two points is derived as the difference between two inertial accelerations at the same two points. Consider here that three SDF accelerometers are set at a certain point P_1 which is l_1 distance away from point P_0 in a vehicle with an inertial acceleration vector $\boldsymbol{\alpha}_0(\alpha_{0x}, \alpha_{0y}, \alpha_{0z})$ and an angular velocity vector $\boldsymbol{\omega}(\omega_x, \omega_y, \omega_z)$ so that their input axes may be turned along the directions of x_1, y_1 and z_1 axes parallel to x, y and z axes, respectively (see Fig.2). Also, consider that another three SDF accelerometers are set at a point P_2, l_2 distance away from point P_0 so that their input axes may be turned along the directions of x_2, y_2 and z_2 axes parallel to x, y and z axes, respectively (see Fig.2). The components of inertial acceleration, gravitational acceleration and size effect in points P_m (m = 1, 2) shown in Fig.2 along the direction of $P_m x_m$, $P_m y_m$, $P_m z_m$ axes (m = 1, 2) are expressed by α_{mi}, g_{mi} and S_{mi} (m = 1, 2, i = x, y, z), respectively. The outputs of accelerometers at point P_m (m = 1, 2) are expressed by a_{mx}, a_{my} and a_{mz}, respectively. Considering that angular velocity (ω_x, ω_y, ω_z), angular acceleration ($\dot{\omega}_x$, $\dot{\omega}_y$, $\dot{\omega}_z$) and inertial acceleration (α_{mi}, m = 0, 1, 2, i = x, y, z) are constant throughout the vehicle, respectively, outputs of six accelerometers at the points P_1 and P_2 are as follows:

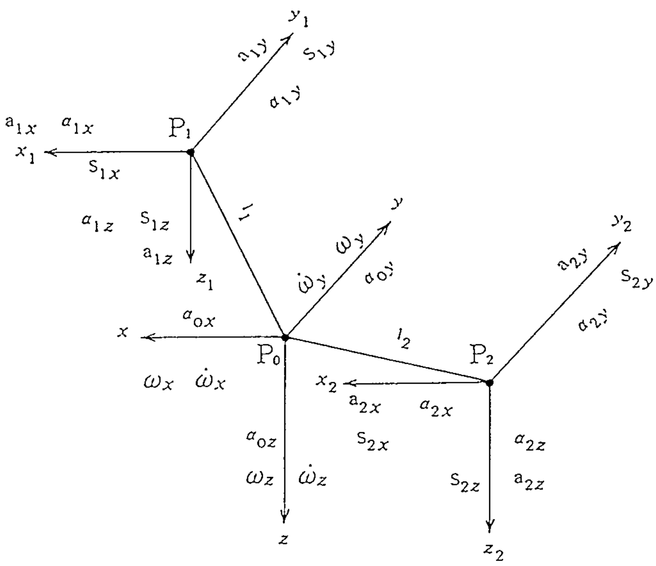

Fig.2 Inertial quantities in points P_0, P_1 and P_2

$$a_{ij}=\alpha_{ij}+S_{ij}-g_{ij}=\alpha_{0j}+S_{ij}-g_{ij},\ i=1, 2,\ j=x, y, z \qquad (7)$$

Here, S_{1j} and S_{2j} are size effect and derived as the following equation[3].

$$\begin{aligned}\mathbf{S}_m &= S_{mx}\mathbf{i}_x + S_{my}\mathbf{i}_y + S_{mz}\mathbf{i}_z \\ &= \dot{\boldsymbol{\omega}} \times \mathbf{l}_m + \boldsymbol{\omega} \times (\boldsymbol{\omega} \times \mathbf{l}_m),\quad m = 1, 2\end{aligned} \qquad (8)$$

$$\mathbf{l}_m = l_{mx}\mathbf{i}_x + l_{my}\mathbf{i}_y + l_{mz}\mathbf{i}_z \qquad (9)$$

Here, $\mathbf{i}_x$, $\mathbf{i}_y$, $\mathbf{i}_z$ are unit vectors along x, y and z directions, respectively. l_{mx}, l_{my} and l_{mz} are the components of the distance l_m (m = 1, 2) along x, y and z directions, respectively. These size effects are obtained using the three-axis angular velocities measured by the gyroscopes and the three-axis angular accelerations measured by the angular accelerometers[5),6)] if the distance between the center of gravity and the point where the accelerometers are installed is known. Line accelerations along the x, y and z axes in points P_1 and P_2 are expressed in the following equations.

$$A_{ij} = a_{ij} - S_{ij} = \alpha_{0j} - g_{ij}\quad i = 1, 2\quad j = x, y, z \qquad (10)$$

The above equations show that the components of the line accelerations are obtained from the measurement data of accelerometers, gyroscopes and angular accelerometers. Moreover, it is clear that the difference between the outputs of two line accelerations in the points P_1 and P_2 is the difference between the gravitational accelerations in the points P_1 and P_2 as shown in the following equation.

$$A_{1j} - A_{2j} = g_{2j} - g_{1j} = \Delta g_j, \quad j = x, y, z \tag{11}$$

Gravity gradients defined in Eq.(4) are obtained applying the above concept to the measurement data of inertial sensors. Additionally, superconducting gravity gradiometer[7),8)] has been developed, taking into consideration such configuration concept.

4. Configuration of Measurement System

Three methods for constructing the measurement system in which SDF, TDF and THDF accelerometers are used, respectively, are shown here. The following assumptions are used in the configuration of the measurement system. (1) The gyroscopes and angular accelerometers are used along with the accelerometers in order to measure three-axis angular velocities and angular accelerations necessary to obtain the size effect, respectively. This means that the size effect contained in the accelerometer outputs is removed using the quantities obtained from the measurement data. (2) Each component of gravity gradients is constant anywhere throughout the vehicle. This means that the variation of gravitational acceleration in a point of the vehicle is linearly dependent on the distance between the point and the center of gravity.

4.1 Gravity Gradiometer Using SDF Accelerometers

A measurement system can be configured by arraying twelve SDF accelerometers as shown in Fig. 3 (a), (b) and (c). The twelve accelerometers are arrayed by 4's so that their input axes are situated on xy, yz and zx planes, respectively. P_{ij} ($i = 1 \sim 3$, $j = 1 \sim 4$) in Fig.3 are the points where the accelerometers are located, and I_{ij} shows the direction of input axis of the accelerometer. Angles θ_{z1} and θ_{z2} about the oz-axis are the angle between the ox-axis and segment $\overline{P_{11}P_{13}}$ and the angle between the oy-axis and segment $\overline{P_{12}P_{14}}$, respectively. Angles θ_{x1} and θ_{x2} about the ox-axis are the angle between the oy-axis and segment $\overline{P_{21}P_{23}}$ and the angle between the oz-axis and segment $\overline{P_{22}P_{24}}$, respectively. Angles θ_{y1} and θ_{y2} about the oy-axis are the angle between the oz-axis and segment $\overline{P_{31}P_{33}}$ and the angle between the ox-axis and segment $\overline{P_{32}P_{34}}$, respectively. l_{ij} is the distance from point P_0 to points P_{ij}. I_{11}, I_{12}, I_{21}, I_{22}, I_{31} and I_{32} are parallel to I_{13}, I_{14}, I_{23}, I_{24}, I_{33} and I_{34}, respectively. This means that the input axes of the accelerometers situated at the points P_{11}, P_{12}, P_{21}, P_{22}, P_{31} and P_{32} are parallel to the input axes of the accelerometers situated at points P_{13}, P_{14}, P_{23}, P_{24}, P_{33} and P_{34}, respectively. Accelerometer output, line and gravitational accelerations and size effect at point P_{ij} are expressed by a_{ij}, A_{ij}, g_{ij} and S_{ij}, respectively. Line acceleration A_{ij} at point P_{ij} is as follows:

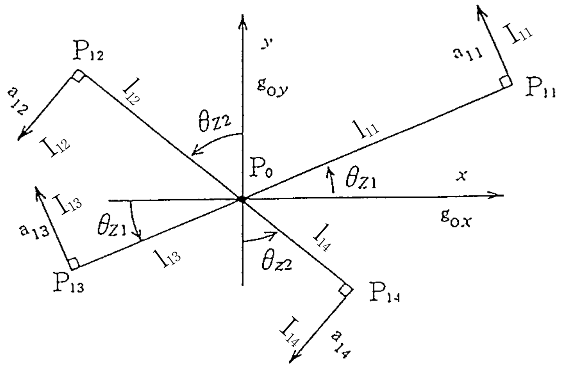

(a) Array on the xy-plane

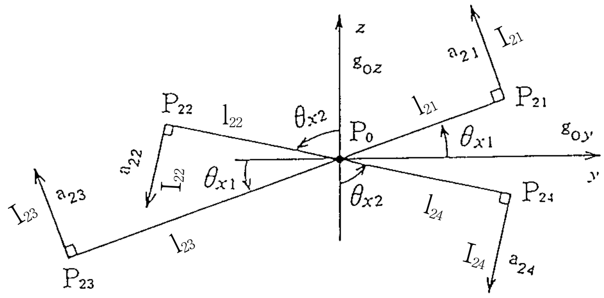

(b) Array on the yz-plane

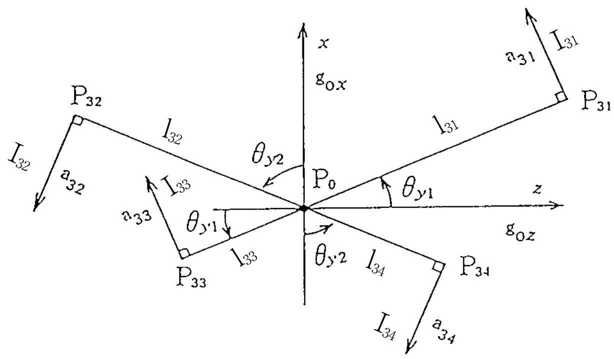

(c) Array on the zx-plane

Fig.3 Array of SDF accelerometers

$$A_{ij} = a_{ij} - S_{ij} = \alpha_{ij} - g_{ij} \tag{12}$$

Here, A_{ij} is regarded as measurement data. α_{ij} is an inertial acceleration of the vehicle. The following relations are derived from Eq.(12) in the same way as Eq.(11) is derived.

$$\left.\begin{aligned}\Delta A_{11} &= A_{11} - A_{13} = g_{13} - g_{11}\\ \Delta A_{12} &= A_{12} - A_{14} = g_{14} - g_{12}\\ \Delta A_{21} &= A_{21} - A_{23} = g_{23} - g_{21}\\ \Delta A_{22} &= A_{22} - A_{24} = g_{24} - g_{22}\\ \Delta A_{31} &= A_{31} - A_{33} = g_{33} - g_{31}\\ \Delta A_{32} &= A_{32} - A_{34} = g_{34} - g_{32}\end{aligned}\right\} \tag{13}$$

The theory that inertial accelerations are the same throughout a vehicle ($\alpha_{i1} = \alpha_{i3}, \alpha_{i2} = \alpha_{i4}, i = 1, 2$) is applied to the derivation of Eq.(13). The components of gravitational acceleration g_0 at the point P_0 along the x, y and z axes are expressed by g_{0x}, g_{0y} and g_{0z}. Then, the relations among the gravitational accelerations $g_{ij}(i = 1 \sim 3, j = 1 \sim 4)$, the components g_{0x}, g_{oy}, g_{0z} of g_0 and gravity gradients $g_{ij}(i,j = x, y, z)$ are as follows:

$$\begin{aligned} g_{11} = &- \{g_{0x} + l_{11}\ (g_{xx} \cos\theta_{z1} + g_{xy} \sin\theta_{z1})\}\ \sin\theta_{z1}\\ &+ \{g_{0y} + l_{11}\ (g_{xy} \cos\theta_{z1} + g_{yy} \sin\theta_{z1})\}\ \cos\theta_{z1}\end{aligned} \tag{14}$$

$$\begin{aligned} g_{12} = &- \{g_{0x} - l_{12}\ (g_{xx} \sin\theta_{z2} - g_{xy} \cos\theta_{z2})\}\ \cos\theta_{z2}\\ &- \{g_{0y} - l_{12}\ (g_{xy} \sin\theta_{z2} - g_{yy} \cos\theta_{z2})\}\ \sin\theta_{z2}\end{aligned} \tag{15}$$

$$\begin{aligned} g_{13} = &- \{g_{0x} - l_{13}\ (g_{xx} \cos\theta_{z1} + g_{xy} \sin\theta_{z1})\}\ \sin\theta_{z1}\\ &+ \{g_{0y} - l_{13}\ (g_{xy} \cos\theta_{z1} + g_{yy} \sin\theta_{z1})\}\ \cos\theta_{z1}\end{aligned} \tag{16}$$

$$\begin{aligned} g_{14} = &- \{g_{0x} + l_{14}\ (g_{xx} \sin\theta_{z2} - g_{xy} \cos\theta_{z2})\}\ \cos\theta_{z2}\\ &- \{g_{0y} + l_{14}\ (g_{xy} \sin\theta_{z2} - g_{yy} \cos\theta_{z2})\}\ \sin\theta_{z2}\end{aligned} \tag{17}$$

$$\begin{aligned} g_{21} = &- \{g_{0y} + l_{21}\ (g_{yy} \cos\theta_{x1} + g_{yz} \sin\theta_{x1})\}\ \sin\theta_{x1}\\ &+ \{g_{0z} + l_{21}\ (g_{yz} \cos\theta_{x1} + g_{zz} \sin\theta_{x1})\}\ \cos\theta_{x1}\end{aligned} \tag{18}$$

$$\begin{aligned} g_{22} = &- \{g_{0y} - l_{22}\ (g_{yy} \sin\theta_{x2} - g_{yz} \cos\theta_{x2})\}\ \cos\theta_{x2}\\ &- \{g_{0z} - l_{22}\ (g_{yz} \sin\theta_{x2} - g_{zz} \cos\theta_{x2})\}\ \sin\theta_{x2}\end{aligned} \tag{19}$$

$$\begin{aligned} g_{23} = &- \{g_{0y} - l_{23}\ (g_{yy} \cos\theta_{x1} + g_{yz} \sin\theta_{x1})\}\ \sin\theta_{x1}\\ &+ \{g_{0z} - l_{23}\ (g_{yz} \cos\theta_{x1} + g_{zz} \sin\theta_{x1})\}\ \cos\theta_{x1}\end{aligned} \tag{20}$$

$$\begin{aligned} g_{24} = &- \{g_{0y} + l_{24}\ (g_{yy} \sin\theta_{x2} - g_{yz} \cos\theta_{x2})\}\ \cos\theta_{x2}\\ &- \{g_{0z} + l_{24}\ (g_{yz} \sin\theta_{x2} - g_{zz} \cos\theta_{x2})\}\ \sin\theta_{x2}\end{aligned} \tag{21}$$

$$\begin{aligned} g_{31} = &- \{g_{0z} + l_{31}\ (g_{zz} \cos\theta_{y1} + g_{zx} \sin\theta_{y1})\}\ \sin\theta_{y1}\\ &+ \{g_{0x} + l_{31}\ (g_{zx} \cos\theta_{y1} + g_{xx} \sin\theta_{y1})\}\ \cos\theta_{y1}\end{aligned} \tag{22}$$

$$\begin{aligned} g_{32} = &- \{g_{0z} - l_{32}\ (g_{zz} \sin\theta_{y2} - g_{zx} \cos\theta_{y2})\}\ \cos\theta_{y2}\\ &- \{g_{0x} - l_{32}\ (g_{zx} \sin\theta_{y2} - g_{xx} \cos\theta_{y2})\}\ \sin\theta_{y2}\end{aligned} \tag{23}$$

$$\begin{aligned} g_{33} = &- \{g_{0z} - l_{33}\ (g_{zz} \cos\theta_{y1} + g_{zx} \sin\theta_{y1})\}\ \sin\theta_{y1}\\ &+ \{g_{0x} - l_{33}\ (g_{zx} \cos\theta_{y1} + g_{xx} \sin\theta_{y1})\}\ \cos\theta_{y1}\end{aligned} \tag{24}$$

$$\begin{aligned} g_{34} = &- \{g_{0z} + l_{34}\ (g_{zz} \sin\theta_{y2} - g_{zx} \cos\theta_{y2})\}\ \cos\theta_{y2}\\ &- \{g_{0x} + l_{34}\ (g_{zx} \sin\theta_{y2} - g_{xx} \cos\theta_{y2})\}\ \sin\theta_{y2}\end{aligned} \tag{25}$$

Above equations are derived based on the assumption that each component of graviy gradient tensor $[g_{ij}](i, j = x, y, z)$ is the same throughout a vehicle. The same assumption is equally applied to other cases in this paper. ΔA_{11} in Eq.(13) is changed in the following form by substituting Eqs.(14) and (16) into Eq.(13).

$$\begin{aligned}\Delta A_{11} &= A_{11} - A_{13} = g_{13} - g_{11}\\ &= l_{z1}\left\{\frac{\sin 2\theta_{z1}}{2}(g_{xx} - g_{yy}) - (\cos 2\theta_{z1})g_{xy}\right\}\\ &= [u_{11}\ u_{12} \cdots u_{16}]\ g^T\end{aligned} \tag{26}$$

$$g = [g_{xx}\ g_{yy}\ g_{zz}\ g_{xy}\ g_{yz}\ g_{zx}] \tag{27}$$

$$l_{z1} = l_{11} + l_{13} = \text{length of } \overline{p_{11}p_{13}} \tag{28}$$

Here, $u_{1j}(j = 1 \sim 6)$ are as follows:
$u_{11} = (l_{z1} \sin 2\theta_{z1})/2,\ u_{12} = -(l_{z1} \sin 2\theta_{z1})/2,$
$u_{13} = u_{15} = u_{16} = 0,\ u_{14} = -l_{z1} \cos 2\theta_{z1}$

$\Delta A_{12}, \Delta A_{21}, \Delta A_{22}, \Delta A_{31}, \Delta A_{32}$ are derived as the function of $g_{ij}(i, j = x, y, z)$ in the same way as the Eq.(26) is derived. The following relation is obtained by applying Eq.(6) to these derived equations.

$$Ug^T = \begin{bmatrix}\Delta A_{11}\\ \Delta A_{12}\\ \Delta A_{21}\\ \Delta A_{22}\\ \Delta A_{31}\\ \Delta A_{32}\\ 0\end{bmatrix} \tag{29}$$

Here, U is a 7 by 6 matrix. The elements $u_{ij}(i = 1 \sim 6, j = 1 \sim 6)$ of U are obtained using lengths of segments $\overline{P_{11}P_{13}}$, $\overline{P_{12}P_{14}}$, $\overline{P_{21}P_{23}}$, $\overline{P_{22}P_{24}}$, $\overline{P_{31}P_{33}}$, $\overline{P_{32}P_{34}}$ $(= l_{z1}, l_{z2}, l_{x1}, l_{x2}, l_{y1}, l_{y2})$ and array angles $\theta_{z1}, \theta_{z2}, \theta_{x1}, \theta_{x2}, \theta_{y1}, \theta_{y2}$. Elements $u_{7j}(j = 1 \sim 6)$ are obtained from Eq.(6). The values of elements $u_{ij}(i = 1 \sim 7, j = 1 \sim 6)$ are as follows:

$$\begin{aligned} &u_{11} = -u_{12} = (l_{z1}/2)\sin 2\theta_{z1},\ u_{14} = -l_{z1} \cos 2\theta_{z1},\\ &u_{21} = -u_{22} = -(l_{z2}/2)\sin 2\theta_{z2},\ u_{24} = l_{z2} \cos 2\theta_{z2},\\ &u_{32} = -u_{33} = (l_{x1}/2)\sin 2\theta_{x1},\ u_{35} = -l_{x1} \cos 2\theta_{x1},\\ &u_{42} = -u_{43} = -(l_{x2}/2)\sin 2\theta_{x2},\ u_{45} = l_{x2} \cos 2\theta_{x2},\\ &u_{51} = -u_{53} = -(l_{y1}/2)\sin 2\theta_{y1},\ u_{56} = -l_{y1} \cos 2\theta_{y1},\\ &u_{61} = -u_{63} = (l_{y2}/2)\sin 2\theta_{y2},\ u_{66} = l_{y2} \cos 2\theta_{y2},\\ &u_{71} = u_{72} = u_{73} = 1\end{aligned}$$

The values of all other elements except the above are zero. Gravity gradients g_{ij} $(i, j = x, y, z)$ are obtained using such parameters and measurement data ($\Delta A_{11}, \Delta A_{12}, \Delta A_{21}, \Delta A_{22}, \Delta A_{31}, \Delta A_{32}$) if the accelerometers are oriented in such a way that assures the existence of the inverse matrix of U^TU.

4.2 Gravity Gradiometer Using TDF Accelerometers

A measurement system can be configured using six TDF accelerometers as shown in Fig.4. Six accelerometers are arrayed so that their input axes are situated on xy , yz and zx planes by 2's, respectively. P_{ij} in Fig.4 $(i=1\sim 3, j=1,2)$ is the position where each TDF accelerometer is located. Segments $\overline{P_{11}P_{12}}$, $\overline{P_{21}P_{22}}$ and $\overline{P_{31}P_{32}}$ intersect at the center of gravity P_0, and determine the directions with angles θ_z, θ_x and θ_y to x, y and z axes on the xy, yz and zx planes, respectively. l_{ij} is the distance between the point P_0 and the point P_{ij}. I_{ijt} and I_{ijn} show the directions of two axes of each accelerometer located at point P_{ij}, respectively. Signs a, g, S and A with suffix ijk $(i=1\sim 3, j=1,2, k=t,n)$ show accelerometer output, gravitational acceleration, size effect and line acceleration along the direction of I_{ijk}, respectively. Line

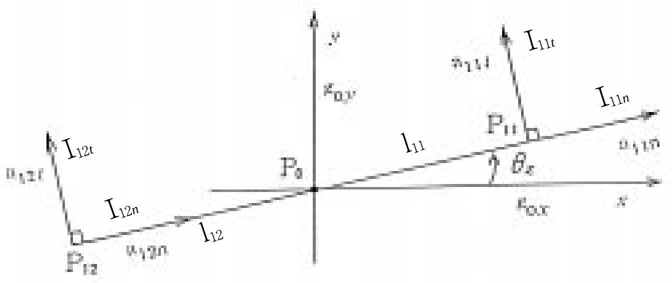

(a) Array on the xy-plane

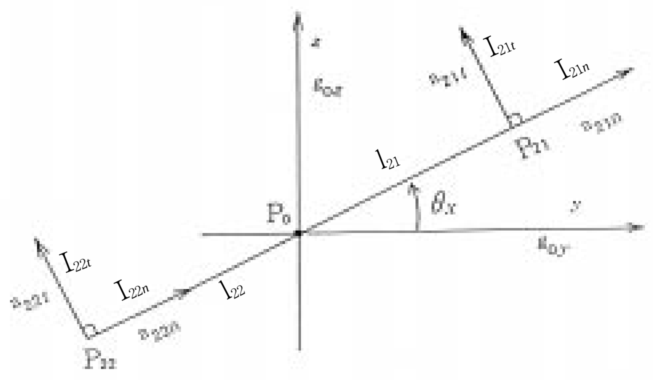

(b) Array on the yz-plane

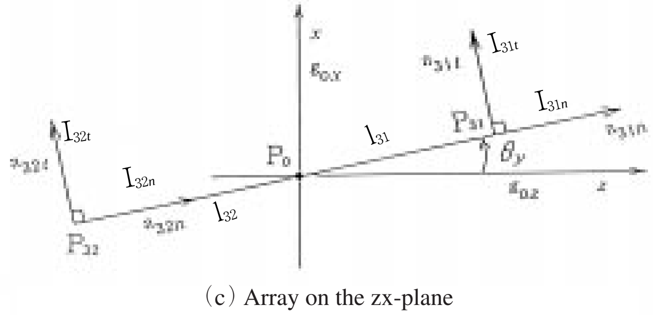

(c) Array on the zx-plane

Fig.4 Array of TDF accelerometers

acceleration A_{ijk} is expressed as follows using the measurement data a_{ijk} and S_{ijk}.

$$A_{ijk} = a_{ijk} - S_{ijk} = \alpha_{ijk} - g_{ijk} \tag{30}$$

The difference between gravitational accelerations at two points some distance from each other is obtained in the same way as Eq.(13) is derived. Accordingly, the following equation is easily derived.

$$\left.\begin{aligned} \Delta A_{1\,k} &= A_{11\,k} - A_{12\,k} = g_{12\,k} - g_{11\,k} \\ \Delta A_{2\,k} &= A_{21\,k} - A_{22\,k} = g_{22\,k} - g_{21\,k} \\ \Delta A_{3\,k} &= A_{31\,k} - A_{32\,k} = g_{32\,k} - g_{31\,k} \end{aligned}\right\} \quad k = t, n \tag{31}$$

Here, the theory that inertial accelerations are the same throughout a vehicle($\alpha_{i1\,t} = \alpha_{i2\,t}$, $\alpha_{i1\,n} = \alpha_{i2\,n}$, $i=1\sim 3$) is applied to the derivation of Eq.(31), also.The gravitational accelerations g_{ijk} $(i=1\sim 3, j=1,2,\ k=t,n)$ can be expressed as the function of components g_{0x}, g_{0y} and g_{0z} of g_0, gravity gradients g_{lm}(l, m = x, y , z), lengths of segments $\overline{P_{11}P_{12}}$, $\overline{P_{21}P_{22}}$, $\overline{P_{31}P_{32}}$ $(=l_1, l_2, l_3)$, distance l_{ijk} and angles θ_z, θ_x, θ_y.

$$\begin{aligned} g_{11\,t} = &-\{g_{0x} + l_{11}\ (g_{xx}\cos\theta_z + g_{xy}\sin\theta_z)\}\ \sin\theta_z \\ &+ \{g_{0y} + l_{11}\ (g_{xy}\cos\theta_z + g_{yy}\sin\theta_z)\}\ \cos\theta_z \end{aligned} \tag{32}$$

$$\begin{aligned} g_{11\,n} = &\{g_{0x} + l_{11}\ (g_{xx}\cos\theta_z + g_{xy}\sin\theta_z)\}\ \cos\theta_z \\ &+ \{g_{0y} + l_{11}\ (g_{xy}\cos\theta_z + g_{yy}\sin\theta_z)\}\ \sin\theta_z \end{aligned} \tag{33}$$

$$\begin{aligned} g_{12\,t} = &-\{g_{0x} - l_{12}\ (g_{xx}\cos\theta_z + g_{xy}\sin\theta_z)\}\ \sin\theta_z \\ &+ \{g_{0y} - l_{12}\ (g_{xy}\cos\theta_z + g_{yy}\sin\theta_z)\}\ \cos\theta_z \end{aligned} \tag{34}$$

$$\begin{aligned} g_{12\,n} = &\{g_{0x} - l_{12}\ (g_{xx}\cos\theta_z + g_{xy}\sin\theta_z)\}\ \cos\theta_z \\ &+ \{g_{0y} - l_{12}\ (g_{xy}\cos\theta_z + g_{yy}\sin\theta_z)\}\ \sin\theta_z \end{aligned} \tag{35}$$

$$\begin{aligned} g_{21\,t} = &-\{g_{0y} + l_{21}\ (g_{yy}\cos\theta_x + g_{yz}\sin\theta_x)\}\ \sin\theta_x \\ &+ \{g_{0z} + l_{21}\ (g_{yz}\cos\theta_x + g_{zz}\sin\theta_x)\}\ \cos\theta_x \end{aligned} \tag{36}$$

$$\begin{aligned} g_{21\,n} = &\{g_{0\,y} + l_{21}\ (g_{yy}\cos\theta_x + g_{yz}\sin\theta_x)\}\ \cos\theta_x \\ &+ \{g_{0z} + l_{21}\ (g_{yz}\cos\theta_x + g_{zz}\sin\theta_x)\}\ \sin\theta_x \end{aligned} \tag{37}$$

$$\begin{aligned} g_{22\,t} = &-\{g_{0y} - l_{22}\ (g_{yy}\cos\theta_x + g_{yz}\sin\theta_x)\}\ \sin\theta_x \\ &+ \{g_{0z} - l_{22}\ (g_{yz}\cos\theta_x + g_{zz}\sin\theta_x)\}\ \cos\theta_x \end{aligned} \tag{38}$$

$$\begin{aligned} g_{22\,n} = &\{g_{0y} - l_{22}\ (g_{yy}\cos\theta_x + g_{yz}\sin\theta_x)\}\ \cos\theta_x \\ &+ \{g_{0z} - l_{22}\ (g_{yz}\cos\theta_x + g_{zz}\sin\theta_x)\}\ \sin\theta_x \end{aligned} \tag{39}$$

$$\begin{aligned} g_{31\,t} = &-\{g_{0z} + l_{31}\ (g_{zz}\cos\theta_y + g_{zx}\sin\theta_y)\}\ \sin\theta_y \\ &+ \{g_{0x} + l_{31}\ (g_{zx}\cos\theta_y + g_{xx}\sin\theta_y)\}\ \cos\theta_y \end{aligned} \tag{40}$$

$$\begin{aligned} g_{31\,n} = &\{g_{0z} + l_{31}\ (g_{zz}\ \cos\theta_y + g_{zx}\sin\theta_y)\}\ \cos\theta_y \\ &+ \{g_{0x} + l_{31}\ (g_{zx}\cos\theta_y + g_{xx}\sin\theta_y)\}\ \sin\theta_y \end{aligned} \tag{41}$$

$$
\begin{aligned}
g_{32t} = &-\{g_{0z} - l_{32}\ (g_{zz}\cos\theta_y + g_{zx}\sin\theta_y)\}\ \sin\theta_y \\
&+ \{g_{0x} - l_{32}\ (g_{zx}\cos\theta_y + g_{xx}\sin\theta_y)\}\ \cos\theta_y
\end{aligned}
\tag{42}
$$

$$
\begin{aligned}
g_{32n} = &\{g_{0z} - l_{32}\ (g_{zz}\cos\theta_y + g_{zx}\sin\theta_y)\}\ \cos\theta_y \\
&+ \{g_{0x} - l_{32}\ (g_{zx}\cos\theta_y + g_{xx}\sin\theta_y)\}\ \sin\theta_y
\end{aligned}
\tag{43}
$$

Thus the following equation is obtained by substituting Eqs.(32) ～(43) into Eq.(31) in the same way as Eq.(29) is derived.

$$
Ug^T = \begin{bmatrix} \Delta A_{1t} \\ \Delta A_{1n} \\ \Delta A_{2t} \\ \Delta A_{2n} \\ \Delta A_{3t} \\ \Delta A_{3n} \\ 0 \end{bmatrix}
\tag{44}
$$

Here, U is a 7 by 6 matrix. The elements $u_{ij}(i, j = 1 \sim 6)$ of U are expressed as the function of array angles θ_z, θ_x, θ_y and lengths of segments $\overline{P_{11}P_{12}}$, $\overline{P_{21}P_{22}}$, $\overline{P_{31}P_{32}}(= l_1, l_2, l_3)$. Elements u_{7j} $(j = 1 \sim 6)$ are obtained from Eq.(6). The values of elements $u_{ij}(i = 1 \sim 7,\ j = 1 \sim 6)$ are as follows:

$u_{11} = -u_{12} = (l_1/2)\sin 2\theta_z$, $u_{14} = -l_1\cos 2\theta_z$,
$u_{21} = -l_1\cos^2\theta_z$, $u_{22} = -l_1\sin^2\theta_z$, $u_{24} = -l_1\sin 2\theta_z$,
$u_{32} = -u_{33} = (l_2/2)\sin 2\theta_x$, $u_{35} = -l_2\cos 2\theta_x$,
$u_{42} = -l_2\cos^2\theta_x$, $u_{43} = -l_2\sin^2\theta_x$, $u_{45} = -l_2\sin 2\theta_x$,
$u_{51} = -u_{53} = -(l_3/2)\sin 2\theta_y$, $u_{56} = -l_3\cos 2\theta_y$,
$u_{61} = -l_3\sin^2\theta_y$, $u_{63} = -l_3\cos^2\theta_y$, $u_{66} = -l_3\sin 2\theta_y$,
$u_{71} = u_{72} = u_{73} = 1$

The values of all other elements except the above are zero. If accelerometers can be arrayed so that the inverse of matrix U^TU exists, the configuration of a gravity gradiometer using TDF accelerometers is possible.

4.3 Gravity Gradiometer Using THDF Accelerometers

A measurement system can be configured using four THDF accelerometers. The pattern of array is very complex as shown in Fig.5. The outline of array-1,2 in Fig.5 is as follows:

① $P_{ij}(i, j = 1, 2)$ is the position where each THDF accelerometer is located.

② Planes $P_0Q_{11}P_{11}U_{11}$ and $P_0Q_{12}P_{12}U_{12}$ are coplanar.
Planes $P_0Q_{21}P_{21}U_{21}$ and $P_0Q_{22}P_{22}U_{22}$ are coplanar.
Segment $\overline{Q_{11}Q_{12}}$ is on the x y-plane.
Segment $\overline{Q_{21}Q_{22}}$ is on the y z-plane.

③ $\overline{Q_{11}P_{11}} \parallel \overline{P_0U_{11}}(= z\text{-axis}) \parallel \overline{P_{12}Q_{12}}$
$\overline{Q_{21}P_{21}} \parallel \overline{P_0U_{21}}(= x\text{-axis}) \parallel \overline{P_{22}Q_{22}}$
$\overline{P_{11}U_{11}} \parallel \overline{Q_{11}Q_{12}} \parallel \overline{U_{12}P_{12}}$
$\overline{P_{21}U_{21}} \parallel \overline{Q_{21}Q_{22}} \parallel \overline{U_{22}P_{22}}$

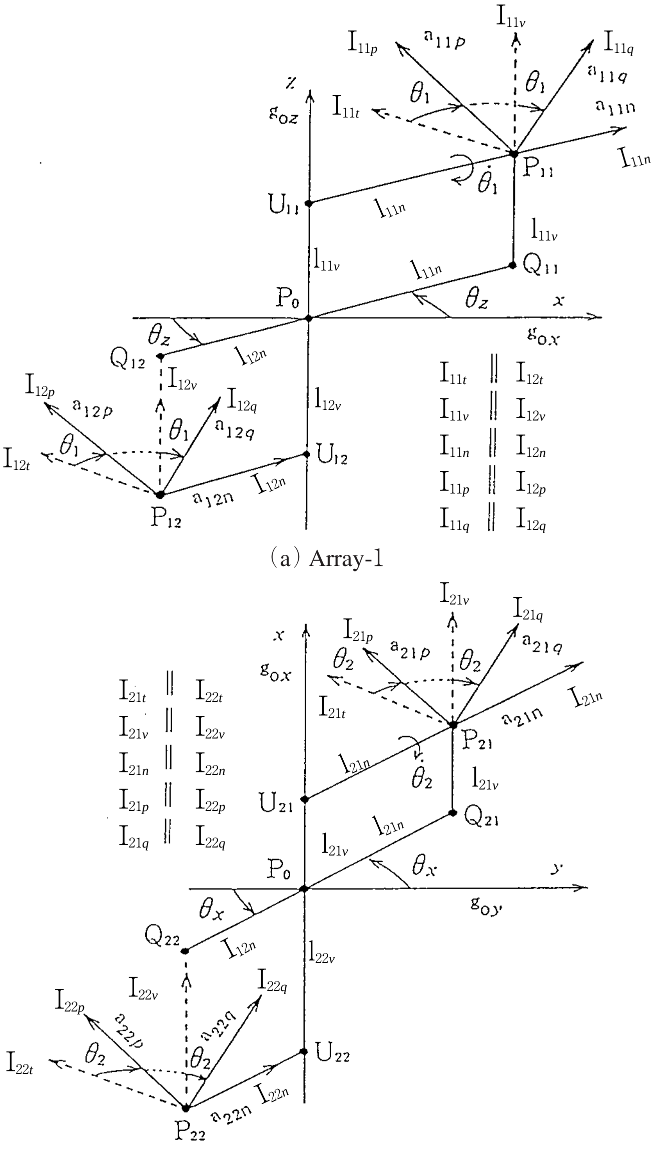

(a) Array-1

(b) Array-2

Fig.5 Array of THDF accelerometers

④ $\angle xP_0Q_{11} = \theta_z$, $\angle yP_0Q_{21} = \theta_x$

Directions of the input axes of the accelerometer located at point P_{11} are shown by I_{11p}, I_{11q} and I_{11n} whose directions are perpendicular to one another. I_{11p}, I_{11q} and I_{11t} are co-planar. Direction I_{11t} is perpendicular to the plane $P_0Q_{11}P_{11}U_{11}$. Direction I_{11n} is equal to the direction of $\overline{U_{11}P_{11}}$. Direction I_{11v} is equal to the direction of $\overline{Q_{11}P_{11}}$. θ_1 is the angle between I_{11p} and I_{11t} which is equal to the angle between I_{11q} and I_{11v}. Directions of the input axes of the accelerometer located at point P_{12}, which are shown by I_{12p}, I_{12q} and I_{12n} in Fig.5(a), are parallel to the directions I_{11p}, I_{11q} and I_{11n}, respectively. The array of the two accelerometers shown in Fig.5(b) is considered to be similar to the array of the two acceleronеters shown in Fig.5(a). I_{21p}, I_{21q} and I_{21n}, which are the directions of the input axes of the accelerometer located at point P_{21}, are parallel to I_{22p}, I_{22q} and I_{22n}, which are the directions of the input axes of the accelerometer located at point P_{22}. x-axis, y-axis and points P_{2i}, Q_{2i}, U_{2i} in array-2 correspond to z-axis, x-axis and points P_{1i}, Q_{1i}, U_{1i}, in array-1 $(i = 1, 2)$, respectively. $I_{2ij}(i = 1, 2,\ j = t, p, v, q, n)$ in Fig.5(b) corresponds to $I_{1ij}(i = 1, 2, j = t, p, v, q, n)$ in Fig.5(a). Inertial acceleration, accelerometer output, gravitational acceleration, size effect and line acceleration along the direction $I_{ijk}(i, j = 1, 2, k = n, p, q)$ are represented by the marks α_{ijk}, a_{ijk}, g_{ijk}, S_{ijk} and A_{ijk}, respectively. Line acceleration A_{ijk} is expressed as follows, using the measurement data a_{ijk} and S_{ijk}.

$$A_{ijk} = a_{ijk} - S_{ijk} = \alpha_{ijk} - g_{ijk} \tag{45}$$

The difference between gravitational accelerations at two points some distance from each other is obtained in the same way as Eq.(13) is derived. Accordingly, the following equation is easily obtained.

$$\begin{aligned}\Delta A_{ik} &= A_{i1k} - A_{i2k}\\ &= g_{i2k} - g_{i1k} \quad i = 1, 2, k = n, p, q\end{aligned} \tag{46}$$

Here, the theory that inertial accelerations are the same throghout a vehicle $(\alpha_{i1p} = \alpha_{i2p}, \alpha_{i1q} = \alpha_{i2q}, \alpha_{i1n} = \alpha_{i2n}, i = 1,2)$ is applied to the derivation of Eq.(46), also. The gravitational accelerations g_{ijn}, g_{ijp} and g_{ijq} $(i, j = 1, 2)$ are expressed as follows using the components g_{0x}, g_{0y} and g_{0z} of g_0, gravity gradients g_{lm} $(l, m = x, y, z)$, array angles $\theta_z, \theta_x, \theta_1, \theta_2$ and distances of segments $\overline{Q_{11}Q_{12}}, \overline{U_{11}U_{12}}, \overline{Q_{21}Q_{22}}, \overline{U_{21}U_{22}} (= l_{1n}, l_{1v}, l_{2n}, l_{2v})$.

$$\begin{aligned}g_{11n} = &\{g_{0x} + l_{11n}(g_{xx}\cos\theta_z + g_{xy}\sin\theta_z) + l_{11v}g_{zx}\}\cos\theta_z\\ &+\{g_{0y} + l_{11n}(g_{xy}\cos\theta_z + g_{yy}\sin\theta_z) + l_{11v}g_{yz}\}\sin\theta_z\end{aligned} \tag{47}$$

$$\begin{aligned}g_{11p} = &-\{g_{0x} + l_{11n}(g_{xx}\cos\theta_z + g_{xy}\sin\theta_z) + l_{11v}g_{zx}\}\sin\theta_z\cos\theta_1\\ &+\{g_{0y} + l_{11n}(g_{xy}\cos\theta_z + g_{yy}\sin\theta_z) + l_{11v}g_{yz}\}\cos\theta_z\cos\theta_1\\ &+\{g_{0z} + l_{11n}(g_{zx}\cos\theta_z + g_{yz}\sin\theta_z) + l_{11v}g_{zz}\}\sin\theta_1\end{aligned} \tag{48}$$

$$\begin{aligned}g_{11q} = &\{g_{0x} + l_{11n}(g_{xx}\cos\theta_z + g_{xy}\sin\theta_z) + l_{11v}g_{zx}\}\sin\theta_z\sin\theta_1\\ &-\{g_{0y} + l_{11n}(g_{xy}\cos\theta_z + g_{yy}\sin\theta_z) + l_{11v}g_{yz}\}\cos\theta_z\sin\theta_1\\ &+\{g_{0z} + l_{11n}(g_{zx}\cos\theta_z + g_{yz}\sin\theta_z) + l_{11v}g_{zz}\}\cos\theta_1\end{aligned} \tag{49}$$

$$\begin{aligned}g_{12n} = &\{g_{0x} - l_{12n}(g_{xx}\cos\theta_z + g_{xy}\sin\theta_z) - l_{12v}g_{zx}\}\cos\theta_z\\ &+\{g_{0y} - l_{12n}(g_{xy}\cos\theta_z + g_{yy}\sin\theta_z) - l_{12v}g_{yz}\}\sin\theta_z\end{aligned} \tag{50}$$

$$\begin{aligned}g_{12p} = &-\{g_{0x} - l_{12n}(g_{xx}\cos\theta_z + g_{xy}\sin\theta_z) - l_{12v}g_{zx}\}\sin\theta_z\cos\theta_1\\ &+\{g_{0y} - l_{12n}(g_{xy}\cos\theta_z + g_{yy}\sin\theta_z) - l_{12v}g_{yz}\}\cos\theta_z\cos\theta_1\\ &+\{g_{0z} - l_{12n}(g_{zx}\cos\theta_z + g_{yz}\sin\theta_z) - l_{12v}g_{zz}\}\sin\theta_1\end{aligned} \tag{51}$$

$$\begin{aligned}g_{12q} = &\{g_{0x} - l_{12n}(g_{xx}\cos\theta_z + g_{xy}\sin\theta_z) - l_{12v}g_{zx}\}\sin\theta_z\sin\theta_1\\ &-\{g_{0y} - l_{12n}(g_{xy}\cos\theta_z + g_{yy}\sin\theta_z) - l_{12v}g_{yz}\}\cos\theta_z\sin\theta_1\\ &+\{g_{0z} - l_{12n}(g_{zx}\cos\theta_z + g_{yz}\sin\theta_z) - l_{12v}g_{zz}\}\cos\theta_1\end{aligned} \tag{52}$$

$$\begin{aligned}g_{21n} = &\{g_{0y} + l_{21n}(g_{yy}\cos\theta_x + g_{yz}\sin\theta_x) + l_{21v}g_{xy}\}\cos\theta_x\\ &+\{g_{0z} + l_{21n}(g_{yz}\cos\theta_x + g_{zz}\sin\theta_x) + l_{21v}g_{zx}\}\sin\theta_x\end{aligned} \tag{53}$$

$$\begin{aligned}g_{21p} = &\{g_{0x} + l_{21n}(g_{xy}\cos\theta_x + g_{zx}\sin\theta_x) + l_{21v}g_{xx}\}\sin\theta_2\\ &-\{g_{0y} + l_{21n}(g_{yy}\cos\theta_x + g_{yz}\sin\theta_x) + l_{21v}g_{xy}\}\sin\theta_x\cos\theta_2\\ &+\{g_{0z} + l_{21n}(g_{yz}\cos\theta_x + g_{zz}\sin\theta_x) + l_{21v}g_{zx}\}\cos\theta_x\cos\theta_2\end{aligned} \tag{54}$$

$$\begin{aligned}g_{21q} = &\{g_{0x} + l_{21n}(g_{xy}\cos\theta_x + g_{zx}\sin\theta_x) + l_{21v}g_{xx}\}\cos\theta_2\\ &+\{g_{0y} + l_{21n}(g_{yy}\cos\theta_x + g_{yz}\sin\theta_x) + l_{21v}g_{xy}\}\sin\theta_x\sin\theta_2\\ &-\{g_{0z} + l_{21n}(g_{yz}\cos\theta_x + g_{zz}\sin\theta_x) + l_{21v}g_{zx}\}\cos\theta_x\sin\theta_2\end{aligned} \tag{55}$$

$$\begin{aligned}g_{22n} = &\{g_{0y} - l_{22n}(g_{yy}\cos\theta_x + g_{yz}\sin\theta_x) - l_{22v}g_{xy}\}\cos\theta_x\\ &+\{g_{0z} - l_{22n}(g_{yz}\cos\theta_x + g_{zz}\sin\theta_x) - l_{22v}g_{zx}\}\sin\theta_x\end{aligned} \tag{56}$$

$$\begin{aligned}g_{22p} = &\{g_{0x} - l_{22n}(g_{xy}\cos\theta_x + g_{zx}\sin\theta_x) - l_{22v}g_{xx}\}\sin\theta_2\\ &-\{g_{0y} - l_{22n}(g_{yy}\cos\theta_x + g_{yz}\sin\theta_x) - l_{22v}g_{xy}\}\sin\theta_x\cos\theta_2\\ &+\{g_{0z} - l_{22n}(g_{yz}\cos\theta_x + g_{zz}\sin\theta_x) - l_{22v}g_{zx}\}\cos\theta_x\cos\theta_2\end{aligned} \tag{57}$$

$$\begin{aligned}g_{22q} = &\{g_{0x} - l_{22n}(g_{xy}\cos\theta_x + g_{zx}\sin\theta_x) - l_{22v}g_{xx}\}\cos\theta_2\\ &+\{g_{0y} - l_{22n}(g_{yy}\cos\theta_x + g_{yz}\sin\theta_x) - l_{22v}g_{xy}\}\sin\theta_x\sin\theta_2\\ &-\{g_{0z} - l_{22n}(g_{yz}\cos\theta_x + g_{zz}\sin\theta_x) - l_{22v}g_{zx}\}\cos\theta_x\sin\theta_2\end{aligned} \tag{58}$$

The right side of Eq.(45), which represents the difference between gravitational accelerations, is expressed as the function of gravity gradients, array angles $\theta_z, \theta_x, \theta_1, \theta_2$ and distances l_{ijn}, $l_{ijv}(i, j = 1, 2)$ in a similar way as Eqs. (29) and (44) are derived. Thus Eq.(46) can be rewritten in the following form.

$$Ug^T = \begin{bmatrix}\Delta A_{1n}\\ \Delta A_{1p}\\ \Delta A_{1q}\\ \Delta A_{2n}\\ \Delta A_{2p}\\ \Delta A_{2q}\\ 0\end{bmatrix} \tag{59}$$

Here, U is a 7 by 6 matrix. The elements $u_{ij}(i, j = 1 \sim 6)$ are expressed as the function of angles $\theta_z, \theta_x, \theta_1, \theta_2$ and distances of segments $\overline{Q_{11}Q_{12}}$, $\overline{U_{11}U_{12}}$, $\overline{Q_{21}Q_{22}}$, $\overline{U_{21}U_{22}} (= l_{1n}, l_{1v}, l_{2n}, l_{2v})$. Elements $u_{7j}(j = 1 \sim 6)$ are obtained from Eq.(6). The values of elements u_{ij} $(i = 1 \sim 7, j = 1 \sim 6)$ are as follows:

$u_{11} = -l_{1n}\cos^2\theta_z$, $u_{12} = -l_{1n}\sin^2\theta_z$, $u_{14} = -l_{1n}\sin 2\theta_z$,
$u_{15} = -l_{1v}\sin\theta_z$, $u_{16} = -l_{1v}\cos\theta_z$,
$u_{21} = -u_{22} = (l_{1n}/2)\sin 2\theta_z\cos\theta_1$, $u_{23} = -l_{1v}\sin\theta_1$,
$u_{24} = -l_{1n}\cos 2\theta_z\cos\theta_1$,
$u_{25} = -l_{1n}\sin\theta_z\sin\theta_1 - l_{1v}\cos\theta_z\cos\theta_1$,
$u_{26} = -l_{1n}\cos\theta_z\sin\theta_1 + l_{1v}\sin\theta_z\cos\theta_1$

$u_{31} = -u_{32} = -(l_{1n}/2)\sin 2\theta_z \sin\theta_1,\ u_{33} = -l_{1v}\cos\theta_1,$
$u_{34} = l_{1n}\cos 2\theta_z \sin\theta_1,$
$u_{35} = -l_{1n}\sin\theta_z\cos\theta_1 + l_{1v}\cos\theta_z\sin\theta_1,$
$u_{36} = -l_{1n}\cos\theta_z\cos\theta_1 - l_{1v}\sin\theta_z\sin\theta_1,$
$u_{42} = -l_{2n}\cos^2\theta_x,\ u_{43} = -l_{2n}\sin^2\theta_x,$
$u_{44} = -l_{2v}\cos\theta_x,\ u_{45} = -l_{2n}\sin 2\theta_x,\ u_{46} = -l_{2v}\sin\theta_x,$
$u_{51} = -l_{2v}\sin\theta_2,\ u_{52} = -u_{53} = (l_{2n}/2)\sin 2\theta_x\cos\theta_2,$
$u_{54} = -l_{2n}\cos\theta_x\sin\theta_2 + l_{2v}\sin\theta_x\cos\theta_2,$
$u_{55} = -l_{2n}\cos 2\theta_x\cos\theta_2,$
$u_{56} = -l_{2n}\sin\theta_x\sin\theta_2 - l_{2v}\cos\theta_x\cos\theta_2$
$u_{61} = -l_{2v}\cos\theta_2,\ u_{62} = -u_{63} = -(l_{2n}/2)\sin 2\theta_x\sin\theta_2,$
$u_{64} = -l_{2n}\cos\theta_x\cos\theta_2 - l_{2v}\sin\theta_x\sin\theta_2,$
$u_{65} = l_{2n}\cos 2\theta_x\sin\theta_2,$
$u_{66} = -l_{2n}\sin\theta_x\cos\theta_2 + l_{2v}\cos\theta_x\sin\theta_2$
$u_{71} = u_{72} = u_{73} = 1$

The values of all other elements except the above are zero. If accelerometers can be arrayed so that the inverse of matrix U^TU exists, the configuration of a gravity gradiometer using THDF accelerometers is possible.

5. Considerations

5.1 A Method of System Configuration

It is desirable to array accelerometers as simply as possible in forming the gravity gradient measurement system. Here, possible formations are shown, considering an intutively clear way to array accelerometers. For example, lengths from point of origin P_0 to the array points of all accelerometers are equal in each configuration of the measurement system using SDF accelerometers.

$$l_{i1} = l_{i2} = l_{i3} = l_{i4}\ (i = 1 \sim 4),$$
$$\theta_1 = \theta_{z1} = \theta_{x1} = \theta_{y1},\quad \theta_2 = \theta_{z2} = \theta_{x2} = \theta_{y2} \tag{60}$$

There exists no inverse matrix of U^TU when $\theta_1 = \theta_2$. But the inverse matrix of U^TU is non-zero if $\theta_1 = 90° - \theta_2$ (for example, $\theta_1 = 30°$, $\theta_2 = 60°$, etc. in $\theta_1 \neq \theta_2$). Similar assumptions are made in the measurement system using TDF accelerometers.

$$l_{i1} = l_{i2}\ (i = 1 \sim 3),\ \theta = \theta_z = \theta_x = \theta_y \tag{61}$$

Thus the inverse matrix of U^TU exists for almost all values of θ (0, 45°, 90°etc.). Similar assumptions are also made in the measurement system using THDF accelerometers.

$$l_{ijn} = l_{ijv}\ (i, j = 1, 2),\ \theta = \theta_z = \theta_x \tag{62}$$

Moreover, $\theta_1 = \theta_2 = 0$ is assumed in order to simplify the configuration. Thus the inverse matrix of U^TU exists for almost all values of θ (0, 45°, 90°etc.).

5.2 An Example of Error Analysis

A quantitative evaluation of the measurement accuracy is shown here. The parameters used for such evaluation are settled as follows in the measurement systems using SDF, TDF and THDF accelerometers, respectively.

$$\left.\begin{array}{l} l_{z1} = l_{z2} = l_{x1} = l_{x2} = l_{y1} = l_{y2} = 1[\mathrm{m}], \\ \theta_{z1} = \theta_{x1} = \theta_{y1} = 60[\mathrm{deg}],\ \theta_{z2} = \theta_{x2} = \theta_{y2} = 30[\mathrm{deg}] \end{array}\right\} \tag{63}$$

$$l_1 = l_2 = l_3 = 1[\mathrm{m}],\ \theta_z = \theta_x = \theta_y = 0\ [\mathrm{deg}] \tag{64}$$

$$l_{1n} = l_{1v} = l_{2n} = l_{2v} = 1[\mathrm{m}],\ \theta_z = \theta_x = \theta_1 = \theta_2 = 0\ [\mathrm{deg}] \tag{65}$$

The measurement accuracy of gravity gradiometer is linearly dependent on the measurement errors of the accelerometers and the variation of the pseudo inverse matrix $\{= (U^TU)^{-1}U^T\}$ caused by the incomplete geometric configuration of the accelerometers, as is obvious from Eqs.(12), (13) and (29) in the array of SDF accelerometers. This discussion is applicable to the measurement accuracy of the gravity gradiometer using TDF or THDF accelerometers. Variation of the size effect is neglected because it is regarded as the second order error (= the variation of error) as shown in Eq.(8). So we assume that the variations of the size effects in Eqs.(12), (30) and (45) are zero. We express Eqs.(29), (44) and (59) by rearranging them as follows:

$$g^T = V\,[\Delta A] = (U^TU)^{-1}U^T\,[\Delta A] \tag{66}$$

$$V = [v_{ij}]\ (i = 1 \sim 6,\ j = 1 \sim 7) = (U^TU)^{-1}U^T \tag{67}$$

Here, ΔA means each right member in Eqs.(29), (44) and (59). Variation of gravity gradient can be expressed as follows:

$$\begin{aligned} \delta g^T &= [\delta g_{xx}\ \delta g_{yy}\ \delta g_{zz}\ \delta g_{xy}\ \delta g_{yz}\ \delta g_{zx}]^T \\ &= \delta V\,[\Delta A] + V\,[\delta(\Delta A)] \end{aligned} \tag{68}$$

Relation between the accelerometer error δa and the variation of gravity gradient δg^T is expressed as follows from Eqs.(12), (30), (45) and (68).

$$\delta g^T \propto \delta(\Delta A) \propto \delta a \tag{69}$$

Here, δa means δa_{ij}, δa_{ijk} and δa_{ijk} in Eqs.(12), (30) and (45), respectively. Errors of all accelerometers are assumed to be statistically same order here. Then , influence of $\delta(\Delta A)$ on δg^T depends on the magnitude of each element v_{ij} ($i = 1 \sim 6$, $j = 1 \sim 6$) of the pseudo inverse matrix V. Ratio of δg_{ij} ($i, j = x, y, z$) to errors of the accelerometers is defined as sensitivity index (= proportional coefficient) in the following form.

$$\delta K_{xx}=\sqrt{\Sigma v_{1j}^2/6},\ \delta K_{yy}=\sqrt{\Sigma v_{2j}^2/6},\ \delta K_{zz}=\sqrt{\Sigma v_{3j}^2/6}$$

$$\delta K_{xy}=\sqrt{\Sigma v_{4j}^2/6},\ \delta K_{yz}=\sqrt{\Sigma v_{5j}^2/6},\ \delta gK_{zx}=\sqrt{\Sigma v_{6j}^2/6}$$

These indexes [1/m] can be obtained from the above-mentioned configuration parameters and are as follows in the system using SDF accelerometes.

$$\delta K_{xx}=\delta K_{yy}=\delta K_{zz}=0.314,\ \delta K_{xy}=\delta K_{yz}=\delta K_{zx}=0.577$$

The indexes are as follows in the system using TDF accelerometers.

$$\delta K_{xx}=\delta K_{yy}=\delta K_{zz}=0.339,\quad \delta K_{xy}=\delta K_{yz}=\delta K_{zx}=0.408$$

The indexes are as follows in the system using THDF accelerometes.

$$\delta K_{xx}=0.272,\quad \delta K_{yy}=\delta K_{zz}=0.379,$$

$$\delta K_{xy}=0.297,\quad \delta K_{yz}=0.360,\ \delta K_{zx}=0.297$$

δV in Eq.(68) shows the influence of incomplete geometric configuration of accelerometers on the measurement accuracy, but the values of its elements are not always proportional to the variations of distances between the locations of two accelerometers and the variations of array angles. Here, incomplete configuration means that there exist such variations of distances or angles. So we define the criterion function of such influence in the following form.

$$\delta V_g=\sqrt{\Sigma\Sigma(v_{pij}-v_{nij})^2}\Big/\sqrt{\Sigma\Sigma v_{nij}^2}$$

v_{pij}: values of v_{ij} obtained considering incompleteness of the geometric configuration of accelerometers

v_{nij}: values of v_{ij} in the state of complete geometric configuration of accelerometers

Relation between the values of δVg and the variations δl_{z1}, $\delta\theta_{z1}$ of distance l_{z1}, angle θ_{z1} in the measurement system using SDF accelerometers is shown in Table 1. Relation between the values of δV_g and the variations δl_1, $\delta\theta_z$ of distance l_1, angle θ_z in the measurement system using TDF accelerometers is shown in Table 2. Relation between the values of δVg and the variations δl_{1n}, δl_{1v}, $\delta\theta_z$, $\delta\theta_1$ of distances l_{1n}, l_{1v}, angles θ_z, θ_1 in the measurement system using THDF accelerometers is shown in Table 3.

Additionally, these error analyses have been conducted here as preliminary trial in order to make the configuration procedure of measurement system concrete. More detailed error analyses will be required with the progress of the system design.

6. An Application of Gravity Gradiometer for Strapdown Inertial Navigation System

Here, in order to verify an applicability of gravity gradiometer for strapdown inertial navigation system, an availability of gravity correction using gravity gradiometer is discussed based on the simulation results. For the purpose of this discussion, it is assumued that the earth is homogeneous and spherical and only

Table 1. Relation between δV_g and δl_{z1} $\delta\theta_{z1}$ in the system using SDF accelerometers

δl_{z1} [m]	δV_g [%]	$\delta\theta_{z1}$ [deg]	δV_g [%]
–0.10	4.358	–0.10	0.197
–0.05	2.085	–0.05	0.099
–0.01	0.403	–0.01	0.020
0.01	0.396	0.01	0.020
0.05	1.919	0.05	0.099
0.10	3.688	0.10	0.198

Table 2. Relation between δV_g and δl_1 $\delta\theta_z$ in the system using TDF accelerometers

δl_1 [m]	δV_g [%]	$\delta\theta_z$ [deg]	δV_g [%]
–0.10	6.228	-0.10	0.183
–0.05	2.968	-0.05	0.091
–0.01	0.572	-0.01	0.018
0.01	0.562	0.01	0.018
0.05	2.713	0.05	0.091
0.10	5.202	0.10	0.183

Table 3 Relation between δVg and δl_{1n} δl_{1V} $\delta\theta_z$ $\delta\theta_1$ in the system using TDF accelerometers

δl_{1n} [m]	δV_g [%]	δl_{1V} [m]	δV_g [%]	$\delta\theta_z$ [deg]	δV_g [%]	$\delta\theta_1$ [deg]	δV_g [%]
–0.10	6.105	–0.10	7.475	–0.10	0.142	–0.10	0.099
–0.05	3.010	–0.05	3.614	–0.05	0.071	–0.05	0.050
–0.01	0.595	–0.01	0.704	–0.01	0.014	–0.01	0.010
0.01	0.592	0.01	0.695	0.01	0.014	0.01	0.010
0.05	2.924	0.05	3.385	0.05	0.071	0.05	0.050
0.10	5.759	0.10	6.557	0.10	0.142	0.10	0.099

Table 4. Vehicle Parameters

Parameter	Value	Unit
Total Weight	8000	kgf
Fuel Weight	6000	kgf
Fuel Consumption	120	kgf/s
Thrust	30000	kgf
Specific Impulse	250	sec

Table 5. Angular Velocities of the Vehicle

Items	Value				Unit
Time	0～3	3～16	16～34	34～58	sec
ω_x	0	0	0	0	deg/sec
ω_y	0	1	0.75	0.6	deg/sec
ω_z	0	0.2	0.3	0.2	deg/sec

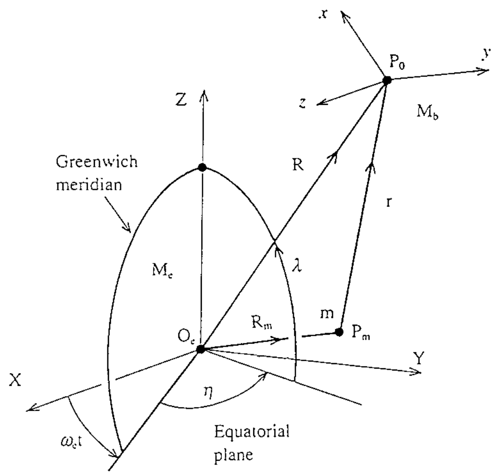

Fig. 6 Positition relation among vehicle, earth and unpredictable body

Table 6. Positions of Unpredictable Bodies

Models	Latitude	Longitude	Altitude	Unit
Model-1	42	14	0	deg
Model-2	40	–110	0	deg
Model-3	28	85	0	deg

the gravitational effects of the earth act on the vehicle, ignoring the small gravity gradient effects of bodies other than the earth, such as the sun, the moon, etc. The simulation is conducted on the assumption that the vehicle using the new type of inertial navigation system composed of gravity gradiometers, accelerometers and gyroscopes moves in the vicinity of the earth.

6.1 Simulation Model

Vehicle parameters are shown in Table 4. Angular velocities ω_x, ω_y, ω_z of the vehicle along the body-fixed axes which are detected by the gyroscopes are shown in Table 5. The outputs of the accelerometers are the components of the vehicle's specific force vector along the body-fixed axes and they are transformed to the components along the navigation reference axes using matrix $[C_{ij}]$ (see Eq.(1)) which is obtained from the outputs of the gyroscopes[9]. The components of the gravitational field g_X, g_Y, g_Z are obtained using Eqs. (A8)～(A14) in appendix, assuming the measurement data of gravity gradients $[g_{ij}]$ $(i, j = x, y, z)$. The vehicle is assumed to be launched toward the east with a launching angle of 45° at the point on the surface where longitude and latitude are 130.970° and 30.399°, respectively. The vehicle is accelerated along the P_0x axis by adding thrust for only 58 seconds from $t = 0$, and it rotates about its own axes (X, Y, Z) with the angular rates shown in Table 5. The vehicle reaches the point of maximum altitude (107 Km) at $t = 250$ sec where longitude and latitude are 141.141° and 30.196°, respectively, and falls at $t = 427$ sec at the point on the surface where longitude is 149.625° and latitude is 29.596°. The necessity for the measurement of gravity gradient arises because of the erratic, unpredictable behavior of the earth's gravitational field vector acting on the vehicle and the difficulty of measuring its deviations from a simple reference model. Here, it is assumed that there exists an unpredictable body with mass "m" at an arbitrary point P_m as shown in Fig. 6. Two kind of gravitational accelerations act on the vehicle. One depends on the earth's mass M_e and the other depends on mass m of the unpredictable body. Accordingly, the potential U_b at point P_0 is derived from equation (2) as follows:

$$U_b = -\mu \frac{1}{R} - \mu_m \frac{1}{r} \tag{70}$$

Here, μ_m is the product of mass m of the unpredictable body with the universal gravitational constant. r is the distance between P_m and P_0, and its components along the navigation reference axes O_eX, O_eY, O_eZ are as follows:

$$r_X = R_X - R_{mX},\ r_Y = R_Y - R_{mY},\ r_Z = R_Z - R_{mZ} \tag{71}$$

Here, R_{mX}, R_{mY} and R_{mZ} are the components of the distance R_m between O_e and P_m along the reference coordinate $O_e - XYZ$. Each element of the gravity gradients for the model shown in

Fig.6 is obtained by substituting U_b in Eq. (71) for U in Eq. (4). It is assumed in the simulation that there exists an unpredictable body at a point near Japan (Model-1) or at a point in the U. S. A. or at a point near the Himalaya on the surface (altitude = 0) as shown in Table 6. That is, the terms "near Japan", "in the U.S.A." and "near the Himalaya" mean the points where the generations of unpredictable bodies are assumed, respectively. The relation between mass m of the unpredictable body and the earth's mass M_e is assumed as follows:

$$m = 10^{-4} M_e, \ M_e \rightarrow M_e - m \qquad (72)$$

The above equation means that the earth's mass is reduced by the quantity of the mass of unpredictable body in the gravity calculatons. Additionally, gravity calculation in the simulation is performed based on the model for measurement of gravity gradients, applying the transformation matrix shown in appendix to the new type of strapdown inertial navigation system using gravity gradiometers,which are newly introduced in this study, along with the gyroscopes and accelerometers which have been used up to the present.

6.2 Simulation Results

Nominal values of gravity gradients $[g_{ij}]$ ($i, j = x, y, z$) are shown in Table 7. These values are obtained by simulation, assuming that there exist no unpredictable bodies. Varied quantities $[\delta g_{ij}]$ ($i, j = x, y, z$) of the nominal values in model-1, model-2 and model-3 are shown in Tables 8, 9 and 10, respectively. It is found from Tables 7 ~ 10 that the accelerometers used in the gravity gradiometers[1),2),7),8)] must be sensitive enough to detect an acceleration variation with the order of 10^{-11} g if they are placed about one meter away from each other. Tables 11, 12 and 13 show the gravity variations δg_N, δg_E, δg_D along the north, east , downrange directions in model-1, model-2 and model-3, respectively. The solid lines of Figs. 7, 8 and 9 show navigation errors caused by the unpredictable body, i.e., variations in the latitude, longitude and altitude, which are expressed by $\delta\lambda$, $\delta\eta$ and δh, respectively. A position variation of one meter on the surface is equivalent to an angle variation of about 10^{-5} deg. $\delta\lambda_c$, $\delta\eta_c$ and δh_c described by dotted lines in Figs. 7, 8 and 9 show the latitude, longitude and altitude errors, respectively, which can not be corrected when the incomplete gravity gradiometer is used. The incomplete gravity gradiometer measures only diagonal elements (g_{xx}, g_{yy}, g_{zz}) of the gravity gradient tensor. It is possible to construct such measurement system using six high-sensitive accelerometers [8]. Accordingly, $\delta\lambda_c$, $\delta\eta_c$ and δh_c are the errors caused by non-diagonal elements of the gravity gradient tensor which are not detected by the gravity gradiometer attainable using current techniqes.

6.3 Availability of Gravity Gradiometer

Comparison between the solid lines and the dotted lines in Figs. 7, 8, 9 shows that it is possible to remove the navigation errors due to an unpredictable body to some degree, though it is impossible to completely remove them. Because the distance between the vehicle's location and the point of the unpredictable body in model-1 (near Japan) is shorter than the one in model-2(

Table 7. Nominal Values of Gravity Gradients (at m = 0)

g_{ij}	t = 50s	100s	200s	300s	400s
g_{xx}	–1394.64	–1425.44	–1287.92	–1136.25	–958.75
g_{yy}	–1519.38	–1489.30	–1458.78	–1465.90	–1511.52
g_{zz}	2914.02	2914.74	2746.69	2602.15	2470.27
g_{xy}	–14.77	–12.46	–22.85	–35.48	–51.29
g_{yz}	–87.47	–101.68	–112.41	–123.97	–137.15
g_{zx}	–748.95	540.13	855.39	1165.17	1490.78

(unit = eötvös = $10^{-9}/s^2$ 10^{-10}g/meter)

Table 8. Variation of Gravity Gradients due to Unpredictable Body (Model-1)

g_{ij}	t = 50s	100s	200s	300s	400s
g_{xx}	1.4153	–0.7130	–11.2185	–16.8058	–8.6397
g_{yy}	5.5992	9.8601	24.3965	33.3205	23.0462
g_{zz}	–7.0145	–9.1471	–13.1780	–16.5147	–14.4065
g_{xy}	11.2879	13.7100	12.0686	–2.2251	–13.3543
g_{yz}	4.2886	–5.2067	–9.0863	–6.5409	1.7335
g_{zx}	–3.6687	–3.6571	–2.8206	0.4127	–0.1668

(unit = eötvös = $10^{-9}/s^2$ 10^{-10}g /meter)

Table 9. Variation of Gravity Gradients due to Unpredictable Body (Model-2)

δg_{ij}	t=50 s	100 s	200 s	300 s	400 s
δg_{xx}	0.0989	0.1080	0.0939	0.0721	-0.0532
δg_{yy}	0.1345	0.1331	0.1424	0.1605	0.1899
δg_{zz}	-0.2334	-0.2411	-0.2364	-0.2326	-0.2431
δg_{xy}	0.0345	0.0395	0.0404	0.0435	0.0487
δg_{yz}	-0.0543	-0.0517	-0.0563	-0.0599	-0.0638
δg_{zx}	-0.1422	-0.1397	-0.1631	-0.2104	-0.2579

(unit = eötvös = $10^{-9}/s^2$ 10^{-10}g/meter)

Table 10. Variation of Gravity Gradients due to Unpredictable Body (Model-3)

δg_{ij}	t=50 s	100 s	200 s	300 s	400 s
δg_{xx}	0.9408	0.7924	0.6376	0.0505	0.3968
δg_{yy}	-0.2529	-0.1985	-0.1223	-0.0674	-0.0262
δg_{zz}	-0.6879	-0.5939	-0.5154	-0.4381	-0.3606
δg_{xy}	- 0.2796	-0.2395	-0.1665	-0.1179	-0.0823
δg_{yz}	-0.0456	-0.0530	-0.0224	0.0009	0.0192
δg_{zx}	0.1567	0.1974	0.0632	-0.0672	-0.1697

(unit = eötvös = $10^{-9}/s^2$ 10^{-10}g/meter)

Table 11. Variation of Gravitational Acceleration due to Unpredictable Body (Model-1)

δg_i	t=50 s	100 s	200 s	300 s	400 s
δg_N	11.0611	13.9056	20.4077	23.6741	20.1890
δg_E	8.3050	8.5515	6.4755	0.1922	-5.9241
δg_D	1.0408	1.6883	2.9914	3.2145	1.9430

(unit=$10^{-3}m/s^2 \fallingdotseq 10^{-4}g$)

Table 12. Variation of Gravitational Acceleration due to Unpredictable Body (Model-2)

δg_i	t=50 s	100 s	200 s	300 s	400 s
δg_N	0.2593	0.2620	0.2703	0.2824	0.2991
δg_E	0.2370	0.2489	0.2789	0.3174	0.3665
δg_D	-0.6272	-0.6136	-0.6104	-0.6418	-0.7142

(unit=$10^{-3}m/s^2 \fallingdotseq 10^{-4}g$)

Table 13. Variation of Gravitational Acceleration due to Unpredictable Body (Model-3)

δg_i	t=50 s	100 s	200 s	300 s	400 s
δg_N	0.2884	0.2804	0.2682	0.2590	0.2511
δg_E	-1.8738	-1.6600	-1.3228	-1.0788	- 0.8946
δg_D	-0.2626	-0.2747	-0.3190	-0.3737	-0.4301

(unit=$10^{-3}m/s^2 \fallingdotseq 10^{-4}g$)

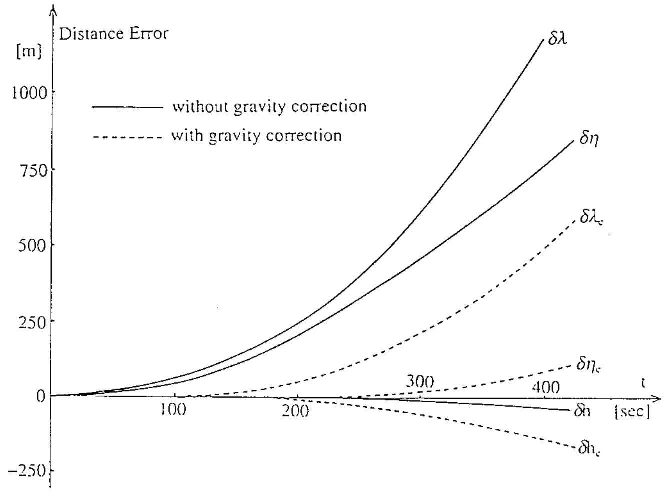

Fig. 7 Navigation errors due to unpredictable body (model-1)

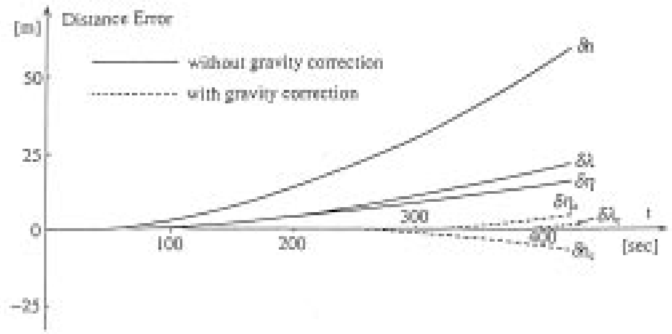

Fig. 8 Navigation errors due to unpredictable body (model-2)

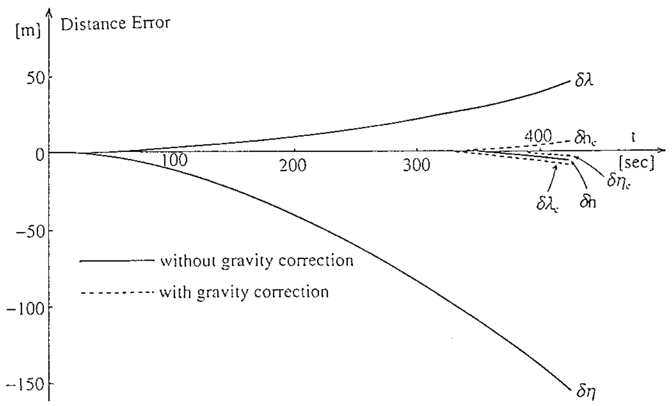

Fig. 9 Navigation errors due to unpredictable body (model-3)

in U.S.A.) and the one in model-3(near the Himalaya), it can be easily understood that the values of the variations of gravity gradients shown in Table 8 are smaller than those shown in Tables 9 and 10. That is, the effect of an unpredictable body on the gravitational potential at any given point of a vehicle is relatively larger when the body is located near the vehicle. Similar tendencies are seen for the variations of gravitational acceleration δg_N, δg_E and δg_D in Tables 11 ∼ 13. and the variations of positions $\delta\lambda$, $\delta\eta$ and δh in Figs. 7, 8, 9. The variations in vertical gravity and position are different from these tendencies. The gravitational potential due to the earth's mass decreases if it is decreased by the amount of the mass of the unpredictable body. The direction of the gravity acceleration vector obtained from the gravity potential of both the earth's mass and the mass of the unpredictable body is almost vertical, because the earth is assumed to be spherical and homogeneous. The vertical gravitational acceleration due to the earth's mass decreases because its mass is assumed to be reduced by the amount of the mass of the unpredictable body. On the other hand, considering the distance between the vehicle's location and the center of the unpredictable body, the increase in vertical gravitational acceleration in model-1(near Japan → near the vehicle) is larger in comparison with those in model-2 and model-3(in the U.S.A. and near the Himalaya → further away from the vehicle). Because the variation of vertical gravity acceleration is the sum of the decrease in gravitational acceleration due to reduction of the earth's mass($M_e \rightarrow M_e - m$, see Eq.(72)) and the increase in gravitational acceleration due to the addition of the mass of the unpredictable body, naturally the variation δg_D in model-1 is larger than the variation δg_D in model-2 or model-3. Two gravity calculation methods are used in the navigation simulation. In one method the gravity is calculated directly, taking into consideration the existense of the unpredictable body. In the other method the gravity is obtained from the simulated data of gravity gradients $[g_{ij}]$ using Eqs. (A8) ∼(A14). It has been found that the results of calculations using these two methods closely agree within the limits of computation accuracy(order of 10^{-10}). Thus, it can be considered that the algorithm shown in Eqs. (A8)∼(A14)is very effective and useful in processing the data obtained from gravity gradiometers. That is, simulation results show that the algorithms shown in Eqs. (A8)∼(A14) can be applied to an advanced strapdown inertial navigation system using gravity gradiometers; thus it is concluded that a fundamental concept for obtaining the gravitational field vector from the measured data of gravity gradients has been established. Moreover, it is shown through the simulation results that the navigation errors due to the variation of gravitational acceleration generated by an unpredictable body can be reduced to some degree even if the incomplete gravity gradiometer, which can detect only the diagonal elements of the gravity gradient tensor, is used. However, in order to detect the variations of gravity gradients shown in Tables 8, 9 and 10, the order of sensitivity of accelerometers used for the gravity gradiometer must be less than 10^{-11}g. Research concerning such highly sensitive "accelerometers" will be required in the future.

7. Conclusions

As a preliminary study concerning the onboard real-time measurement of the gravitational field with a view to reducing the influence of the gravity anomaly[4),7)] on navigation performance, a fundamental concept for both the configuration of a gravity gradient measurement system using twelve SDF or six TDF or four THDF accelerometers and the applicability of such measurement system for strapdown inertial navigation system has been established. And also, it has been verified that the navigation errors caused by the gravity anomaly can be remarkably reduced even if the incomplete gravity gradiometer, which is realizable using current techniques, is used. A gravity gradiometer can be constructed by the mixed use of SDF, TDF, THDF accelerometers, and various types of measurement systems in accordance with the mission requirements will be possible. If an inertial navigation system with high sensitive gravity gradiometers could be realized, the navigation errors of the vehicle due to gravity uncertainties would be reduced remarkably, within the limits of such presently ignored phenomena as geographical effects,etc. and no pre-mission surveying of the gravitational field would be required. However, in order to realize such an advanced inertial navigation system, "accelerometers" used as the components of gravity gradiometers must be so highly sensitive that the gravity gradients can be detected as the difference between the outputs of the accelerrometers[1),2),7)]. Additionally, a gravity gradiometer can be useful not only for the construction of a high-performance inertial navigation system but also for the study on geophysics, geodesy, mineral exploration, etc. [2),7),10)]

References

1) Gerber, M. A., 'Gravity Gradiometry, Astronautics & Aeronautics', pp. 18-26, May 1978
2) Morgan, S. H. and Paik, H. J., 'Superconducting Gravity Gradiometer Mission', NASA TM-4091, 1989
3) Hung, J. C., Hunter, J. S. and White, H. V., 'SIZE EFFECT IN INERTIAL MEASUREMENT SYSTEMS', FAC Control Science and Technology, pp. 2259–2264, 1981

4) Britting, K. R., 'Inertial Navigation Systems Analysis', John Wiley & Sons, Inc., pp. 49–64, 1971

5) Shingu, H. and Otsuki, M., 'Noninteracting Control of Dynamically Tuned Dry Gyro and Its Application to Measurement of Two-axis Angular Accelerations', Preprints of the XIth IFAC Symposium on Automatic Control in Aerospace, pp. 171–176, 1989

6) Suzuki, T., Nagayasu, M. and Sasa, S., 'Status and Trends in Angular Accelerometers', Journal of Japan Society for Aeronautical and Space Sciences (in Japanese), Vol. 38, No. 433, pp.102-109, February 1990

7) Paik, H. J. and Leung J-S., 'Global Gravity Survey by an Orbiting Gravity Gradiometer', Transactions of American Geophysical Union, Vol. 69, No. 48, pp.69–48, November 1988

8) Paik, H. J. and Richard, J–P., 'Development of a Sensitive Superconducting Gravity Gradiometer for Geological and Navigation Application', NASA CR-4011, 1986

9) Broxmeyer, C., 'Inertial Navigation Systems' McGraw-Hill, pp. 21–34, 1964

10) Shingu, H., 'An Algorithm for Gravity Calculations in Strapdown Inertial Navigation Using Gravity Gradiometers', Proceedings of the 7 th Symposium on Guidance and Control for Aerospace, SICE, pp. 45–54, 1990

Appendix

An Algorithm for Gravity Calculations in Strapdown Inertial Navigation System Using Gravity Gradiometers

The process of obtaining the gravitational accelerations from the measured data of gravity gradients is analytically shown in this appendix.The values of the gravity gradients measured by gravity gradiometers in strapdown use are expressed as the components of a spatial gradient of the gravity along the body-fixed coordinate axes. To obtain the gravitational acceleration acting on the vehicle, these values must be transformed to components along the navigation reference coordinate axes. The transformation matrix, that is, an algorithm necessary to transform the components of gravity gradients measured on a moving vehicle to the components along the navigation reference coordinate axes, is derived through analysis of the gravitational field. The outputs of gravity gradiometers in strapdown use are the quantities for the elements of matrix $[g_{nm}]$ in Eq.(4). In order to solve the strapdown inertial navigation equation, it is necessary to transform the values of these outputs to the components of matrix $[g_{ij}]$ $(i, j = X, Y, Z)$ in Eq. (3) along the navigation reference axes. If the inverse of matrix $[C_{ij}]$ in Eq. (1) is defined such that

$$[B_{ij}] = \begin{bmatrix} B_{11} & B_{12} & B_{13} \\ B_{21} & B_{22} & B_{23} \\ B_{31} & B_{32} & B_{33} \end{bmatrix} = [C_{ij}]^{-1} = \begin{bmatrix} C_{11} & C_{12} & C_{13} \\ C_{21} & C_{22} & C_{23} \\ C_{31} & C_{32} & C_{33} \end{bmatrix}^{-1} \quad \text{(A1)}$$

then, the relations shown in Eq. (1) are as follows:

$$[R_x\ R_y\ R_z]^T = [B_{ij}]\,[R_X\ \ R_Y\ \ R_Z]^T \quad \text{(A2)}$$

The relations between the components along the body-fixed coordinate and the components along the reference coordinate of the gravitational field vector are as follows:

$$[g_X\quad g_Y\quad g_Z]^T = [C_{ij}][g_x\quad g_y\quad g_z]^T \quad \text{(A3)}$$

$$[g_x\quad g_y\quad g_z]^T = [B_{ij}]\,[g_X\quad g_Y\quad g_Z]^T \quad \text{(A4)}$$

The spatial gradients of the gravitational accelerations g_X, g_Y, g_Z along the K direction $(K = X, Y, Z)$ are derived as follows from Eqs.(1), (4), (A1)～(A4).

$$g_{XK} = \frac{\partial g_X}{\partial R_K} = C_{11}\frac{\partial g_x}{\partial R_K} + C_{12}\frac{\partial g_y}{\partial R_K} + C_{13}\frac{\partial g_z}{\partial R_K}$$

$$= [C_{11}\ C_{12}\ C_{13}]\,[g_{ij}]\,[B_{1K}\ B_{2K}\ B_{3K}]^T \quad \text{(A5)}$$

$$g_{YK} = \frac{\partial g_Y}{\partial R_K} = C_{21}\frac{\partial g_x}{\partial R_K} + C_{22}\frac{\partial g_y}{\partial R_K} + C_{23}\frac{\partial g_z}{\partial R_K}$$

$$= [C_{21}\ C_{22}\ C_{23}]\,[g_{ij}]\,[B_{1K}\ B_{2K}\ B_{3K}]^T \quad \text{(A6)}$$

$$g_{ZK} = \frac{\partial g_Z}{\partial R_K} = C_{31}\frac{\partial g_x}{\partial R_K} + C_{32}\frac{\partial g_y}{\partial R_K} + C_{33}\frac{\partial g_z}{\partial R_K}$$

$$= [C_{31}\ C_{32}\ C_{33}]\,[g_{ij}]\,[B_{1K}\ B_{2K}\ B_{3K}]^T \quad \text{(A7)}$$

Here, K in $[B_{1K}\ B_{2K}\ B_{3K}]^T$ is 1, 2 and 3, respectively, corresponding to X, Y and Z of K in g_{XK}, g_{YK}, g_{ZK} and R_K. It is found from Eqs. (A5)～(A7) that each element of the gravity gradient g_{lk} ($l, K = X, Y, Z$) along the reference coordinate is obtained if the measurement data $[g_{ij}]$ $(i, j = x, y, z)$ are transformed using the following relation.

$$[g_{lk}] = \begin{bmatrix} g_{XX} & g_{XY} & g_{XZ} \\ g_{YX} & g_{YY} & g_{YZ} \\ g_{ZX} & g_{ZY} & g_{ZZ} \end{bmatrix} = [C_{ij}] \begin{bmatrix} g_{xx} & g_{xy} & g_{xz} \\ g_{yx} & g_{yy} & g_{yz} \\ g_{zx} & g_{zy} & g_{zz} \end{bmatrix} [B_{ij}] \quad \text{(A8)}$$

$$i, j = 1, 2, 3$$

The components of the gravitational acceleration are obtained by spatial integral calculation for the gravity gradients:

$$g_X = \int g_{XX}\,dR_X + \int g_{XY}dR_Y + \int g_{XZ}dR_Z \quad \text{(A9)}$$

$$g_Y = \int g_{YX}\,dR_X + \int g_{YY}dR_Y + \int g_{YZ}dR_Z \quad \text{(A10)}$$

$$g_Z = \int g_{ZX}\,dR_X + \int g_{ZY}dR_Y + \int g_{ZZ}dR_Z \quad \text{(A11)}$$

However, navigation equations are usually solved through time integral. g_X, g_Y, g_Z may be generally obtained through the following equations using the vehicle velocities V_X, V_Y, V_Z along the reference coordinate axes because dR_X, dR_Y and dR_Z are $V_X dt$, $V_Y dt$ and $V_Z dt$, respectively.

$$g_X = \int g_{XX}\,V_X dt + \int g_{XY}V_Y dt + \int g_{XZ}V_Z\,dt \quad \text{(A12)}$$

$$g_Y = \int g_{YX}\,V_X dt + \int g_{YY}V_Y dt + \int g_{YZ}V_Z\,dt \quad \text{(A13)}$$

$$g_Z = \int g_{ZX}\,V_X dt + \int g_{ZY}V_Y dt + \int g_{ZZ}V_Z\,dt \quad \text{(A14)}$$

As mentioned above, it is possible to calculate gravitational accelerations in real time on a moving vehicle, if the measured data of gravity gradients are transformed to the components along reference coordinate axes using Eq.(A8), and these transformed data are applied to Eqs. (A12)～(A14).

TECHNICAL REPORT OF NATIONAL AEROSPACE LABORATORY
TR-1333T

航空宇宙技術研究所報告 1333T 号（欧文）

平 成 9 年 9 月 発 行

発 行 所　科 学 技 術 庁 航 空 宇 宙 技 術 研 究 所
東京都調布市深大寺東町７丁目44番地１
電 話 （０４２２）４７－５９１１ 〒１８２
印 刷 所　株 式 会 社　東 京 プ レ ス
東 京 都 板 橋 区 桜 川 ２ － 27 － 12

Published by
NATIONAL AEROSPACE LABORATORY
7-44-1 Jindaiji higashi, Chōfu, Tokyo 182
JANAPN

Printed in Japan